AAS 01-382

TARGETING OF PRECESSION MANEUVER WITH ACTIVE NUTATION CONTROL

Sergei Tanygin*

Simultaneous precession maneuver and active nutation control has been proposed recently for axisymmetric spinners. The proposed method modifies nominal start and stop times of each pulse during the precession maneuver in order to reduce residual nutation while maintaining precession accuracy. This paper examines several open- and closed-loop approaches to refining the original solution via targeting. Parametric studies indicate significant accuracy improvements as well as potential fuel savings.

INTRODUCTION

Spin stabilization remains a preferred option for many small spacecraft. A number of larger spacecraft are also spinning at least during some phase of their lifetime[1-4]. During spinning, the spacecraft reorientation is accomplished using precession maneuver. This involves pulsing the offset axial thruster at times when the applied torque can move the angular momentum vector in the desired direction. This induces nutation of the axisymmetric spacecraft, which moves its spin axis. With the appropriate choice of inertia moments, the nutation can be cancelled by the end of the maneuver and spacecraft placed into a pure spin about its new inertial orientation.[2,4] If inertia moments do not have certain ratios, the nutation will not be fully cancelled and can actually increase significantly. [5-7] Rigid oblate spinners and prolate spinners may require active nutation control (ANC) to cancel residual nutation.[4] One recently proposed method modifies start and stop times of each pulse during the precession maneuver to reduce the residual nutation while maintaining precession accuracy for a wide range of inertia moments.[5,7] Accomplishing this can lead to a better pointing accuracy as well as fuel and time savings. This paper seeks to improve the performance of the original method by incorporating closed-loop corrections and differential corrections for adjusting start and stop times. The next section closely follows treatment in Ref.7, whereas subsequent sections describe the proposed improvements.

* Member AAS and AIAA. Lead Engineer, Attitude Dynamics and Control, Analytical Graphics, Inc., 40 General Warren Blvd., Malvern, PA 19355, stanygin@stk.com

SIMULTANEOUS PRECESSION MANEUVER AND ACTIVE NUTATION CONTROL

The method applies to ideally axisymmetric spin-stabilized spacecraft that is required to undergo precession maneuver. The goal of this maneuver is to re-orient both the angular momentum vector and the spin axis so that at the end of the maneuver the latter achieves the desired new orientation and the spacecraft is placed in the pure spin. This can be accomplished by pulsing the axial offset thruster during short intervals of time when direction of the induced torque aligns closely with the desired change in the angular momentum vector. However, for axisymmetric or asymmetric spacecraft, each pulse will also induce nutation, which will generally pull the spacecraft out of the pure spin. For certain ratios of inertia moments of axisymmetric spacecraft, it is possible to pulse every spin period (or multiples of it) to achieve near cancellation of residual nutation at the end of the maneuver. The method proposed in Ref.7 develops formula for small adjustments of start and stop times of each pulse in order to achieve this near cancellation for a wider range of inertia moment ratios. The formula is based on closed form transition for both angular velocity vector and the direction of the spin axis after each pulse cycle. It is assumed that thrust pulses are ideal square waves and the thruster is aligned perfectly with the spin axis. It is also assumed that the spacecraft is axisymmetric, however, no special requirements are imposed on its inertia moments. The notation in this section follows closely the notation used in Ref.7. The oblateness parameter indicates degree of asymmetry of the spacecraft:

$$\sigma \equiv I_a / I_t , \tag{1}$$

where I_a and I_t are the axial and the transverse moments of inertia, respectively. The parameter is greater than 1 for an oblate spacecraft (e.g. disc shaped) and is less than 1 for a prolate spacecraft (e.g. rod shaped). Values farther away from 1 in either direction indicate a more asymmetric spacecraft. Oblateness of 1 corresponds to a symmetric spacecraft (e.g. sphere). The body observed nutation frequency indicates how fast the angular velocity vector is seen rotating about the angular momentum vector:

$$\lambda \equiv (\sigma - 1)\Omega , \tag{2}$$

where Ω is the spin rate about spacecraft's axis of symmetry (or spin axis). That same motion observed in the inertial frame has frequency $\lambda + \Omega = \sigma\Omega$. A thruster located on the side of the spacecraft and firing along the spin axis passes through its desired precession alignment every integer number of spin periods. Any multiplicity of spin periods can be used as the pulse cycle period:

$$T \equiv 2\pi k / \Omega , \; k = 1,2,3,... , \tag{3}$$

but the fastest and simplest strategy calls for pulsing during every revolution of the spacecraft, i.e. $k = 1$. All pulses are assumed to have the same duration Δt, which does not need to be small in derivations below. However, given that the same thrust impulse

$$I_F \equiv F\Delta t\,, \tag{4}$$

where F is the magnitude of the resultant force, is more effective if produced during shorter pulses, a useful simplification can be obtained for $|\Omega\Delta t| << 1$. The derivations in this section seek to decouple the motion of the spin axis from the spin itself. In doing so, a shorthand notation for two-dimensional parameterization of the former is convenient. The two-dimensional vector of transverse angular velocity components is denoted as $\boldsymbol{\omega} \equiv \begin{bmatrix}\omega_1 & \omega_2\end{bmatrix}^{\mathrm{T}}$. Another two-dimensional vector contains angles, which define the spin axis direction. The vector is introduced as $\boldsymbol{\theta} \equiv \begin{bmatrix}\theta_1 & \theta_2\end{bmatrix}^{\mathrm{T}}$, where the angles are collected from the $\theta_2 - \theta_1 - \theta_3$ Euler sequence. Finally, two-dimensional (planar) counterclockwise rotation is mechanized via the following operator

$$\mathbf{R}\{\alpha\} \equiv \begin{bmatrix}\cos\alpha & -\sin\alpha \\ \sin\alpha & \cos\alpha\end{bmatrix}, \tag{5}$$

where α is the angle of rotation.

Another parameter is introduced:

$$\boldsymbol{\omega}_{\mathbf{p}} \equiv \frac{\sigma}{(\sigma-1)h_a}\mathbf{R}\left\{\frac{\pi}{2}\right\}\mathbf{M}\,, \tag{6}$$

which represents the influence of two-dimensional vector of transverse torque components, $\mathbf{M} \equiv \begin{bmatrix}M_1 & M_2\end{bmatrix}^{\mathrm{T}}$, on the transverse angular acceleration $\dot{\boldsymbol{\omega}}$, where $h_a \equiv I_a\Omega$ is the axial angular momentum.

The attitude motion during any given pulse cycle is broken into three phases. The first phase precedes the pulse and the last phase succeeds it. The ith pulse cycle starts at time t_{i-1} with its pre-pulse phase nominally running until $t_{i-1,*} \equiv t_{i-1} + t_* - \Delta t/2$ and post-pulse phase nominally starting at $t_{*,i} \equiv t_{i-1,*} + \Delta t$. The next pulse starts at $t_i \equiv t_{i-1} + T$. The nominal mid-time of the pulse, t_*, is the same within each pulse cycle. Without loss of generality, the pulse can be positioned in the middle of each cycle, $t_* \equiv T/2$, thus, introducing convenient symmetry into the problem. This is possible because the start time of the first pulse can be always adjusted so that the pulses initiate desired precession. The fundamental idea of the proposed method consists of adding small time adjustments, δt_i, to each pulse, such that the adjustment simultaneously moves ith pulse start time, $t_{i-1,\delta} \equiv t_{i-1,*} + \delta t_i$, and its stop time, $t_{\delta,i} \equiv t_{*,i} + \delta t_i$, thus, preserving the pulse duration, Δt.

During each phase, the angular velocity can be integrated in closed-form. The transverse torque only affects the transverse angular velocity components, which are found as follows:[5-7]

$$\boldsymbol{\omega}(t) = \mathbf{R}\{\lambda(t - t_{i-1})\}\boldsymbol{\omega}_{\mathbf{i-1}},\ t_{i-1} \le t \le t_{i-1,\delta},\ \boldsymbol{\omega}_{\mathbf{\iota-1,\delta}} \equiv \boldsymbol{\omega}(t_{i-1,\delta}), \tag{7}$$

$$\boldsymbol{\omega}(t) = \mathbf{R}\{\lambda(t - t_{i-1,\delta})\}(\boldsymbol{\omega}_{\mathbf{i-1,\delta}} - \boldsymbol{\omega}_{\mathbf{p}}) + \boldsymbol{\omega}_{\mathbf{p}},\ t_{i-1,\delta} < t \le t_{\delta,i},\ \boldsymbol{\omega}_{\mathbf{\delta,\iota}} \equiv \boldsymbol{\omega}(t_{\delta,i}), \tag{8}$$

$$\boldsymbol{\omega}(t) = \mathbf{R}\{\lambda(t - t_{\delta,i})\}\boldsymbol{\omega}_{\mathbf{\delta,i}},\ t_{\delta,i} < t \le t_i,\ \boldsymbol{\omega}_{\mathbf{\iota}} \equiv \boldsymbol{\omega}(t_i). \tag{9}$$

Their evolution spanning all three phases is a piecewise smooth function of time, which will be further used to solve for attitude kinematics.

Ability to approximate attitude motion in closed-form depends greatly on the choice of attitude parameterization. Judicious selection of non-symmetrical Euler angle sequence "precession-deviation-spin" facilitates development of the closed-form attitude solution during the precession maneuver. Without loss of generality, let the precession be defined about the reference inertial i_2 axis and the deviation be defined about the precessing (but not spinning) a_1 axis. This way the deviation can be interpreted as the angle between the spin axis and the precession plane. Finally, the spin angle is defined about the body e_3 axis, which is consistent with the selection of the axial angular velocity component. This sequence of Euler angles is not only convenient geometrically, but also permits linearization of the attitude kinematics using only one small angle assumption.[1,4] Namely, the deviation is assumed small, which is reasonable as the proposed method seeks to minimize it. Thus, the linearized attitude kinematics become[7]

$$\dot{\boldsymbol{\theta}}(t) \approx \mathbf{R}\{\Omega t\}\boldsymbol{\omega}(t),\ \theta_1 << 1. \tag{10}$$

The resulting approximate Euler angle derivatives are piecewise integrable in closed-form.

$$\boldsymbol{\theta}_{\mathbf{i}} \equiv \boldsymbol{\theta}(t_i)\ ,\ \boldsymbol{\theta}_{\mathbf{i-1}} \equiv \boldsymbol{\theta}(t_{i-1})$$

$$\boldsymbol{\theta}_{\mathbf{i}} = \boldsymbol{\theta}_{\mathbf{i-1}} + \int_{t_{i-1}}^{t_{i-1,\delta}} \mathbf{R}\{\Omega t\}\boldsymbol{\omega}(t)dt + \int_{t_{i-1,\delta}}^{t_{\delta,i}} \mathbf{R}\{\Omega t\}\boldsymbol{\omega}(t)dt + \int_{t_{\delta,i}}^{t_i} \mathbf{R}\{\Omega t\}\boldsymbol{\omega}(t)dt \tag{11}$$

This formula along with the formula for the transverse angular velocity (Eqs.6-8) can be rewritten as functions of the adjustment, δt_i, and in this form will represent a single pulse cycle state transition equation[7]

$$\mathbf{x}_{\mathbf{i}} = \mathbf{A}_{\mathbf{0}}\mathbf{x}_{\mathbf{i-1}} + (\mathbf{B}_{\mathbf{0}} + \mathbf{B}_{\mathbf{t}}\delta t_i)\boldsymbol{\omega}_{\mathbf{p}} + o(\delta t_i^2), \tag{12}$$

where the state is defined as $\mathbf{x}_{\mathbf{i}} \equiv \begin{bmatrix} \boldsymbol{\theta}_{\mathbf{i}} \\ \boldsymbol{\omega}_{\mathbf{i}} \end{bmatrix}$, the matrices are constructed as $\mathbf{A}_{\mathbf{0}} \equiv \begin{bmatrix} \mathbf{E} & \mathbf{A}_{\boldsymbol{\theta 0}} \\ \mathbf{0} & \mathbf{A}_{\boldsymbol{\omega 0}} \end{bmatrix}$, $\mathbf{B}_{\mathbf{0}} \equiv \begin{bmatrix} \mathbf{B}_{\boldsymbol{\theta 0}} \\ \mathbf{B}_{\boldsymbol{\omega 0}} \end{bmatrix}$, $\mathbf{B}_{\mathbf{t}} \equiv \begin{bmatrix} \mathbf{B}_{\boldsymbol{\theta t}} \\ \mathbf{B}_{\boldsymbol{\omega t}} \end{bmatrix}$ and their exact form can be found in Ref.7. Straightforward

repeated application of the single pulse cycle transition results in the following N pulse cycle transition equation: [7]

$$\mathbf{x_N} = \mathbf{A_0^N x_0} + \sum_{j=0}^{N-1} \mathbf{A_0^j B_0 \omega_p} + \sum_{j=0}^{N-1} \mathbf{A_0^j B_t \omega_p} \delta t_{N-j} + o(\delta t_k \delta t_l)\,,\ k,l = 1,2,...,N\,, \qquad (13)$$

where $\mathbf{x_0}$ is the initial state. This transition equation relates the initial state with the state after N pulse cycles and serves as the basis for the solution developed in Ref.7. Given the desired target state after N pulse cycles, $\hat{\mathbf{x}}_\mathbf{N}$, the adjustment vector $\boldsymbol{\delta t_N} \equiv \left[\delta t_{1N} \quad \delta t_{2N} \quad ... \quad \delta t_{NN}\right]^{\mathrm{T}}$ is sought such that $\mathbf{x_N} \to \hat{\mathbf{x}}_\mathbf{N}$. The approximate minimum-norm solution of Ref.7 is recalled below in the form representing initial iteration of a differential corrector:

$$\boldsymbol{\delta t_N} = {}^{+}\boldsymbol{\Phi}_\mathbf{N} \mathbf{y_N}\,, \qquad (14)$$

where $\mathbf{y_N} \equiv \mathbf{y_N}(\boldsymbol{\delta t} = \mathbf{0}) \equiv \hat{\mathbf{x}}_\mathbf{N} - \mathbf{x_N}(\boldsymbol{\delta t} = \mathbf{0})$ is the target vector and ${}^{+}\boldsymbol{\Phi}_\mathbf{N}$ denotes a pseudo-inverse of the Jacobian

$\boldsymbol{\Phi}_\mathbf{N} \equiv \boldsymbol{\Phi}_\mathbf{N}(\boldsymbol{\delta t} = \mathbf{0}) \equiv \left.\dfrac{\partial \mathbf{x_N}}{\partial \boldsymbol{\delta t}}\right|_{\boldsymbol{\delta t} = \mathbf{0}}$. The pseudo-inverse is computed using a "thin" form of singular value decomposition (SVD), which permits inversion of rank-deficient matrices.[7,8] The N pulse transition equation (Eq.(13)) also provides analytic formulae the state after N nominal pulses[7]

$$\mathbf{x_N}(\boldsymbol{\delta t} = \mathbf{0}) = \mathbf{A_0^N x_0} + \sum_{j=0}^{N-1} \mathbf{A_0^j B_0 \omega_p}\,. \qquad (15)$$

and for the Jacobian evaluated with nominal pulses[7]

$$\boldsymbol{\Phi}_\mathbf{N} \equiv \left[\varphi_{\mathbf{1N}} \quad \varphi_{\mathbf{2N}} \quad ... \quad \varphi_{\mathbf{NN}}\right], \qquad (16)$$

where

$$\varphi_{\mathbf{NN}} \equiv \mathbf{B_t \omega_p}\,, \qquad (17)$$

$$\varphi_{\mathbf{mN}} \equiv \mathbf{A_0} \varphi_{\mathbf{m+1,N}}\,,\ m = 1,2,...,N-1. \qquad (18)$$

DIFFERENTIAL CORRECTOR

The main goal of this study is to refine analytical solutions developed earlier[7] using several targeting schemes. Refinement may be needed because of approximations used in the development of the analytical solutions, e.g. linearization with respect to the time adjustments δt_i and with respect to the deviation angle θ_1. In general, these approximations

will cause the actual target state not be reached precisely. However, formulations of the previous section can be straightforwardly placed within the differential corrector framework. A basic idea of the differential corrector is to pre-multiply target vector by the Jacobian inverse to update the desired adjustment vector. The target vector and the Jacobian are then recomputed using the updated adjustment vector and the procedure is repeated (Fig. 1). The procedure is stopped if either the target vector or the updates to the adjustment vector reach specified vicinity of zero. In addition, it can be stopped if the number of iterations exceeds a pre-imposed limit.

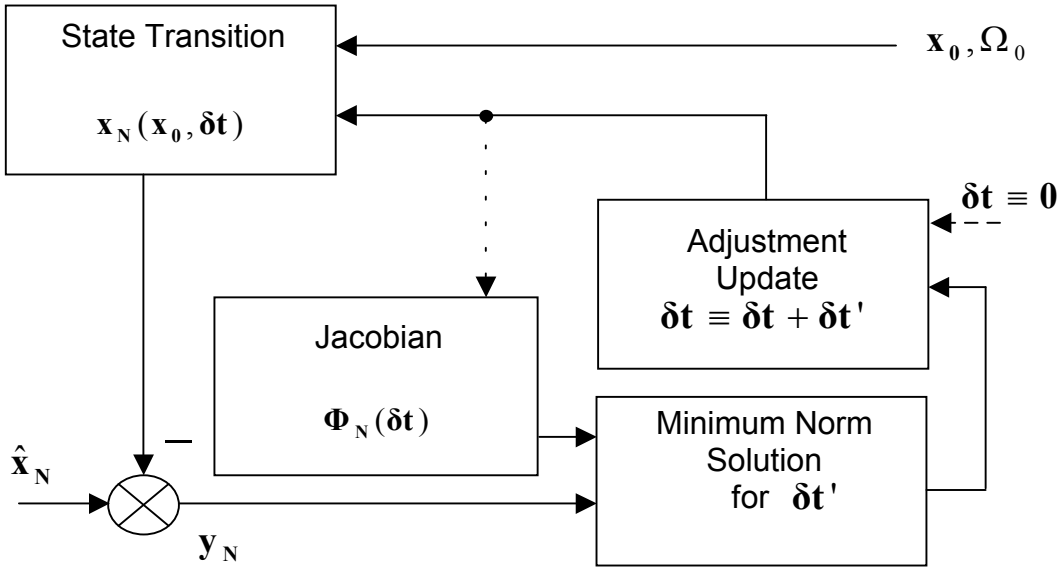

Figure 1 Generic Differential Corrector

A variety of implementations for the differential corrector can be considered. They differ based on the following criteria: how the state is transitioned through the precession maneuver and how as well as how often the Jacobian is updated.

The state can be transitioned either analytically using Eq.(13), semi-analytically using angular velocity transition from Eq.(13) with numerical integration of kinematics or numerically using integration of both angular velocities and kinematics. While analytical approach is generally the fastest, its accuracy suffers from using kinematics linearized with respect to the deviation angle θ_1. The full numerical approach is generally the slowest of the three, but is more accurate then the analytical approach. Also, unlike the analytical or the semi-analytical approaches, the full numerical integration permits accurate state transition even for imperfect near-axisymmetric models. It is possible that even on-board computers should be able to run such numerical integrations faster than real time, which is why this approach was selected for this study.

Computation of the Jacobian can be done also either analytically using Eqs.(16-18) or numerically using perturbations and numerical differencing. However, unlike the state

transition, the analytical approach appears to be favorable for the Jacobian computation. The reason is that, while the numerical approach still represents approximation, it can be also prohibitively expensive computationally. Indeed, this approach would require perturbing every time adjustment at least once (or twice for central differencing) and numerically transitioning state from the corresponding pulse cycle to the end of the maneuver. As the number of time adjustments equals to the number of pulses, the number of numerical runs can be quite large (e.g. ~100 or at least ~10s). Thus, computational cost of the analytical approach is generally much smaller. Another issue related to the computational efficiency of the differential corrector is how often to re-compute the Jacobian. Two limiting cases are to never re-compute the Jacobian, i.e. to use the original Jacobian evaluated with no adjustments, and to re-compute it as often as the adjustment vector is updated. Note that, in practice, large adjustments are undesirable as they mean that the angular momentum vector does not travel along the precession arc, which reduces the overall efficiency of pulses. This means that only solutions with small time adjustments are practical, for which the Jacobian evaluated without time adjustments should be a good approximation of the actual Jacobian. In addition, the differential corrector is typically tolerant to imperfections of the Jacobian, provided that the target vector is close to be linear with respect to the time adjustments, which is the case. These arguments prompted the selection of the analytical approach for the Jacobian computation in this study. Also, this computation is done only once and is based on the nominal pulsing.

A particular implementation of the differential corrector used in this study is depicted in Figure 2.

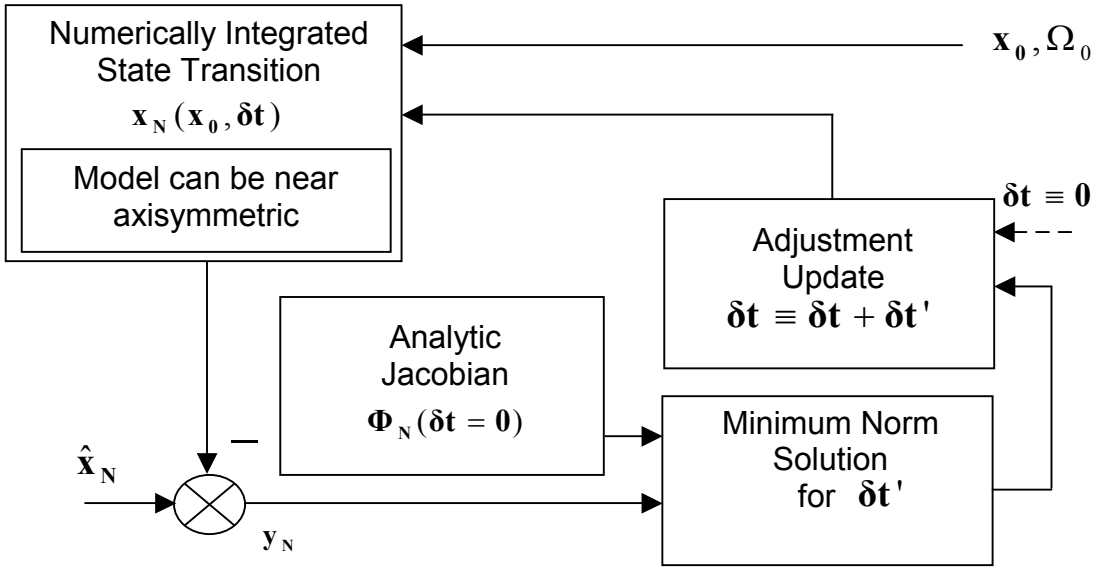

Figure 2 Implemented Differential Corrector

KINEMATICS CORRECTOR

The differential corrector described in the previous section seeks to reduce the residual nutation and the deviation angle after performing N pulses in the course of the precession maneuver. The corrector produces the adjustment vector that contains start time adjustments for each pulse. In the special case, when the maneuver is initiated from the pure spin, it is possible to compute one additional correction, which can completely cancel the deviation angle provided that the axisymmetric model is accurate. This correction is based on using dihedral angle measured between the final orientation of the spin axis and the desired precession plane about the initial spin axis direction. Starting the precession maneuver in the desired plane, i.e. $\theta_{10} \equiv 0$, and from pure spin, i.e. $\omega_{10} \equiv \omega_{20} \equiv 0$, means that the overall start time of the maneuver can be adjusted without affecting its nutation cancellation properties. Changing the overall start time will effectively mean rotating the entire maneuver trajectory about the initial spin axis direction. Given the dihedral angle and the spin rate it is possible to compute the time correction that should place the final state exactly on the precession plane, thus, reducing the final deviation angle to zero (Fig.3).

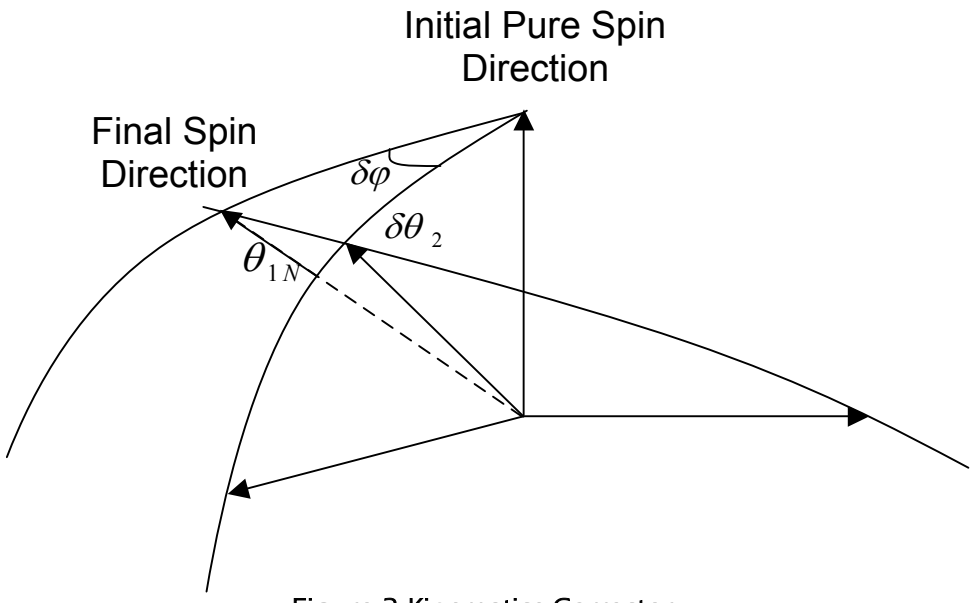

Figure 3 Kinematics Corrector

Spherical geometry based on Figure 3 yields the following formula:

$$\delta\varphi \equiv \tan^{-1}(\tan\theta_{1N} / \sin\delta\theta_2), \tag{19}$$

where $\delta\theta_2 \equiv \theta_{2N} - \theta_{20}$. The additional time adjustment $\delta t'' = \delta\varphi / \Omega_0$ applied to every pulse will cause the desired rotation of the entire maneuver trajectory (Fig.4). This technique can be used with any differential corrector approach.

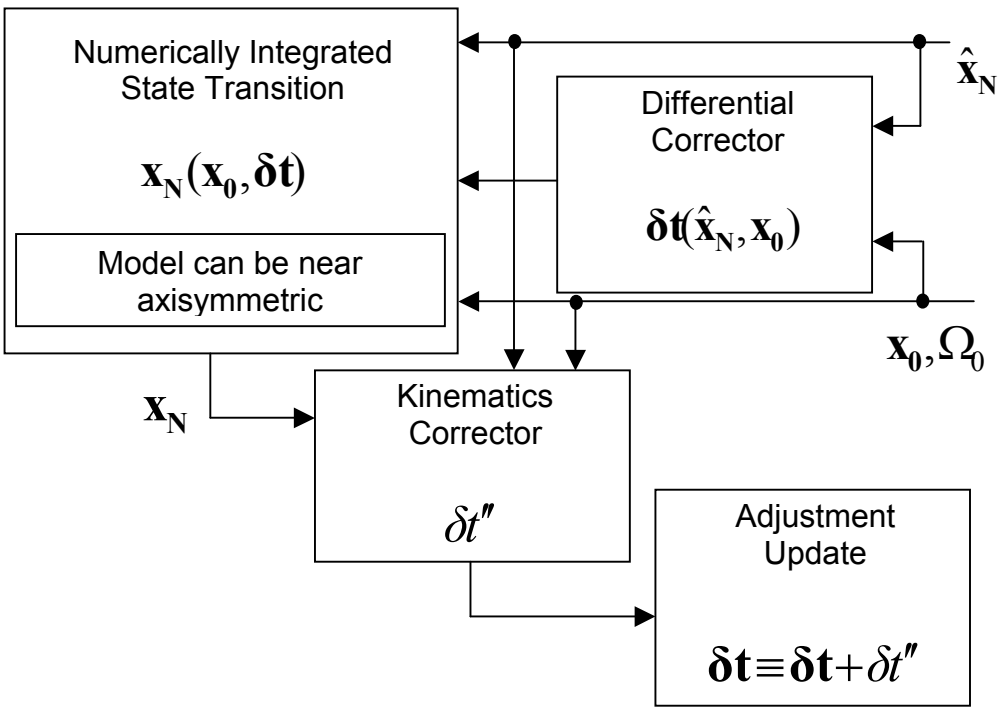

Figure 4 Open-Loop Predictor-Corrector

CLOSED-LOOP SOLVER

All computations employed in the previous sections rely on an a priori information, i.e. no measurements of the state during the maneuver are used. This means that any modeling errors in the state transition are not corrected and can directly affect the maneuver accuracy. If measurements of the state are available during the maneuver, a conceptually simple way to incorporate them is to re-solve the entire targeting problem after every pulse cycle. This closed-loop solver will produce a new adjustment vector after every pulse. Out of this vector only the first (the upcoming) adjustment will be applied and the process is repeated after the pulse cycle is completed. It is likely that, as the number of remaining pulses becomes smaller towards the end of the maneuver, re-solving the problem may produce adjustments that are too large. In order to prevent this behavior, the closed-loop solver may be switched to an open-loop solver some number of pulses before the end of the maneuver (Fig.5).

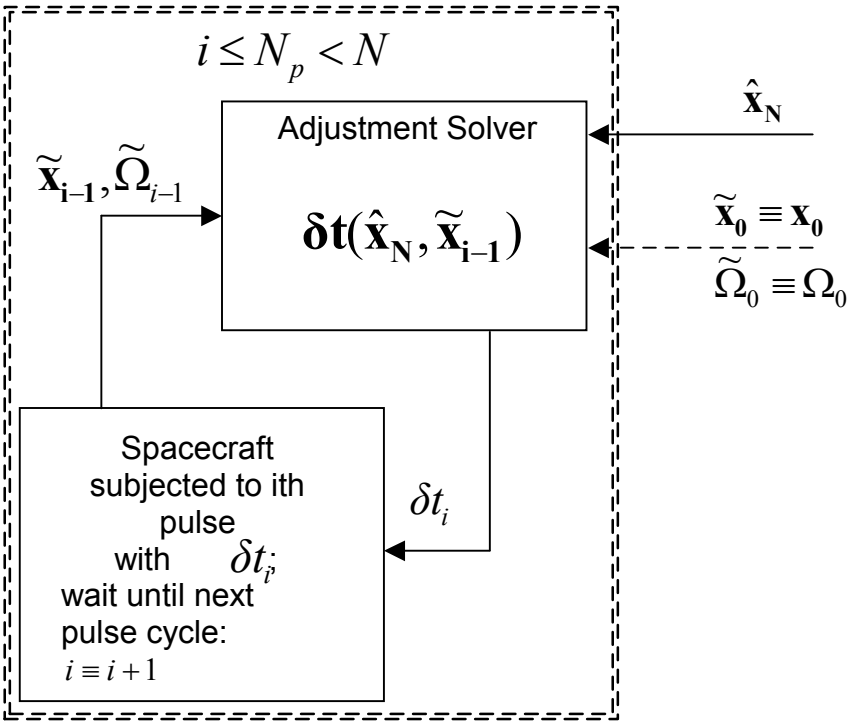

Figure 5 Closed-Loop Solver

PARAMETRIC STUDIES

All studies presented in this paper use the following specification: precession maneuver arc of 20 deg; axial moment of inertia, $I_a = 1$; spin rate, $\Omega = 120$ deg/s; pulse duration Δt such that $\Omega \Delta t = 5$ deg; spacecraft is initially in pure spin. A number of oblateness parameter values are considered, which cover the interval from 0.5 to 2.0. Also the number of pulses varies from 4 to 100. Closed-loop solver is examined for a near-axisymmetric spacecraft with actual transverse moments of inertia different by 5 % from the ones used in the solver, i.e. the actual inertia moments are $1.05 I_t$, $0.95 I_t$ and I_a. This study is done for a 50 pulse maneuver with the switch from closed- to open-loop occurring after 40 pulses. Overall performance in every case agrees with the one seen in Ref.7, however, it should be noted that the differential corrector is generally more successful at reducing residual nutation and deviation angles for a wider range of oblateness parameters especially for relatively small number of pulses. Examination of the closed-loop solver for a set of three oblateness parameter values shows that it can improve precession accuracy even in the presence of mass property imperfections. However, at least in one case, deviation angle actually increased after application of the closed-loop adjustments. This indicates that a more detailed study must be done to evaluate performance of the closed-loop solver.

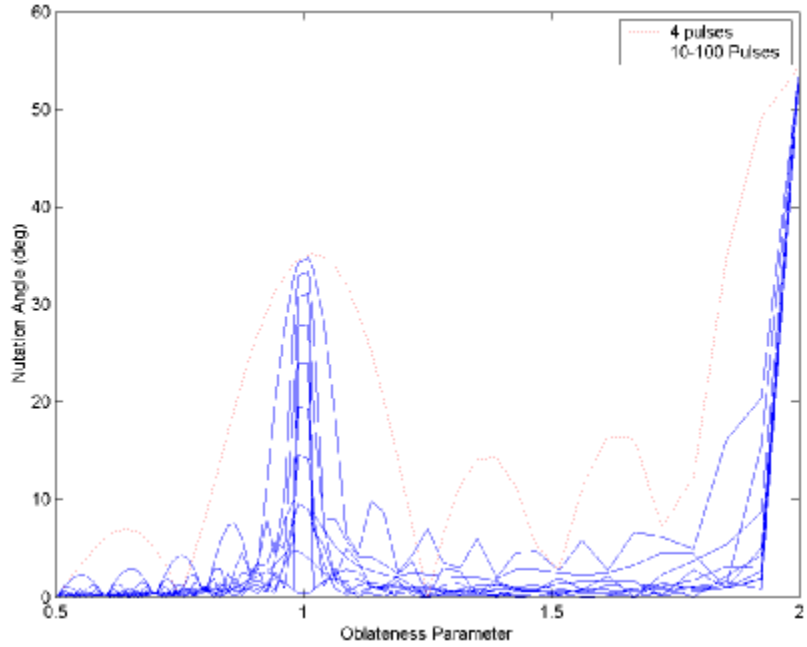

Figure 6 Residual Nutation with Nominal Pulses, deg

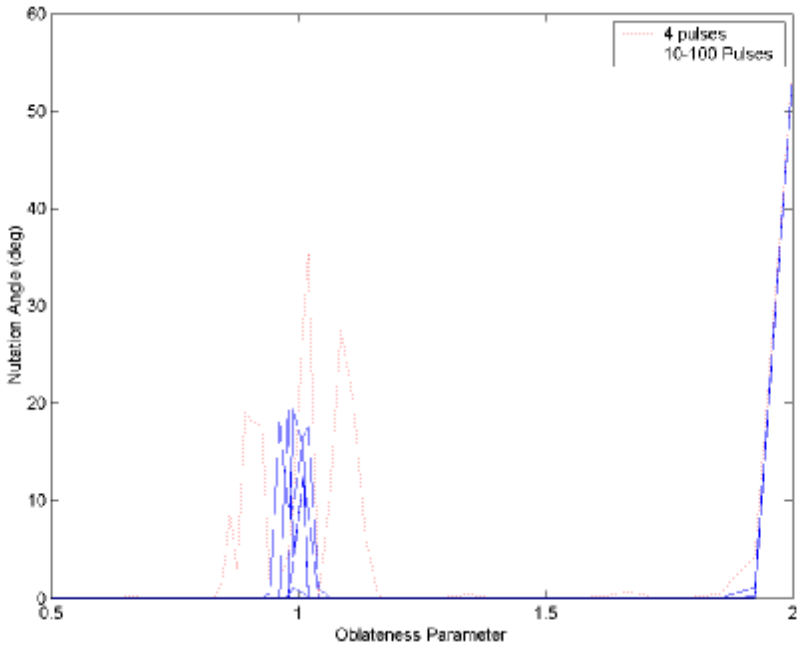

Figure 7 Residual Nutation with Adjusted Pulses, deg

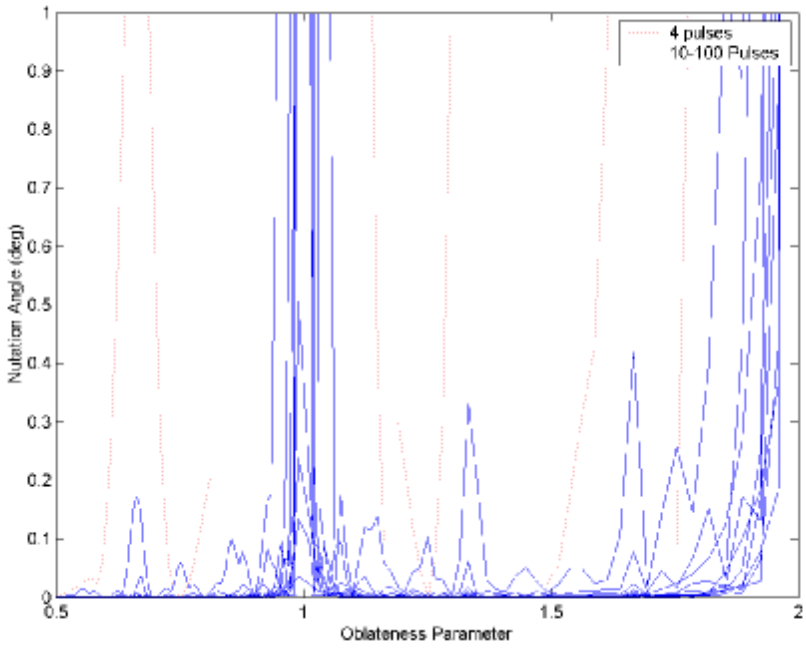

Figure 8 Residual Nutation with Adjusted Pulses (Details), deg

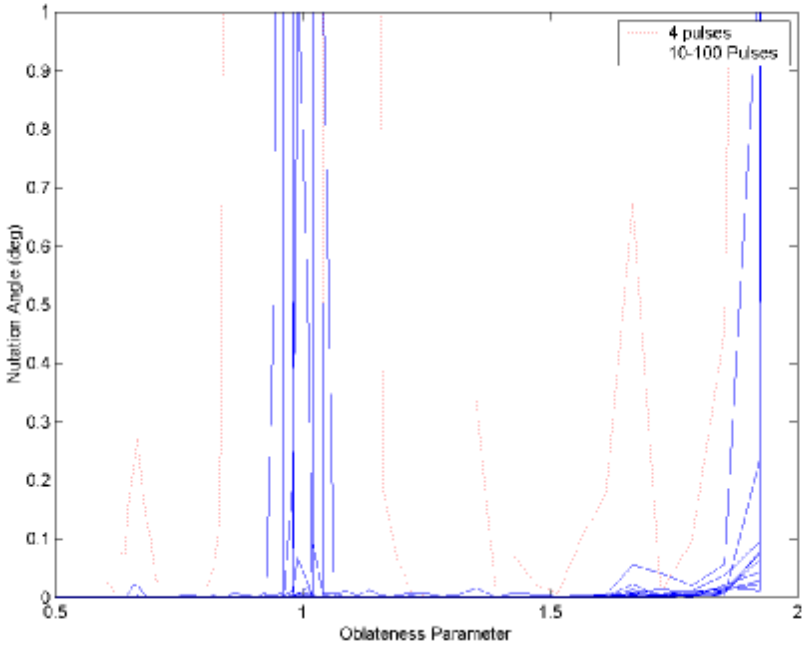

Figure 9 Residual Nutation with Diff. Corrector Adjusted Pulses (Details), deg

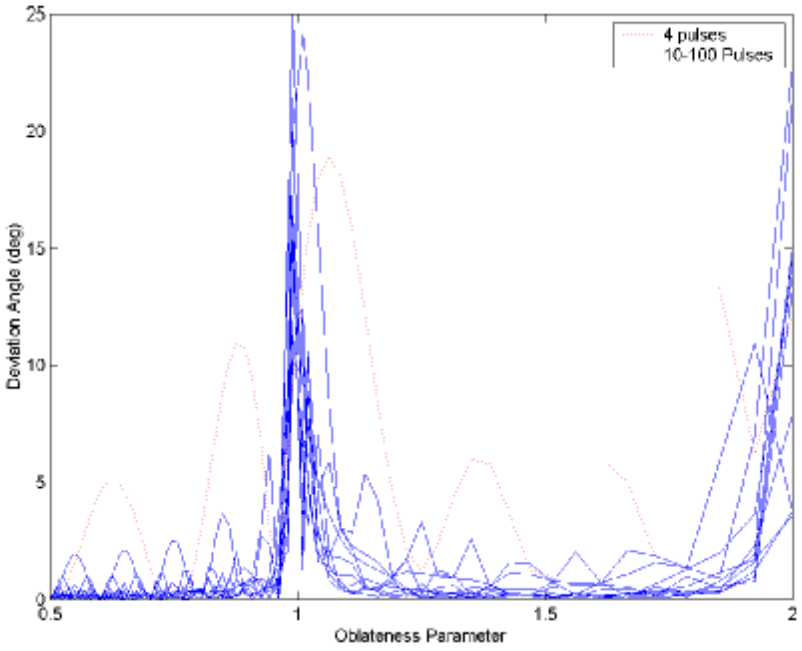

Figure 10 Residual Deviation with Nominal Pulses, deg

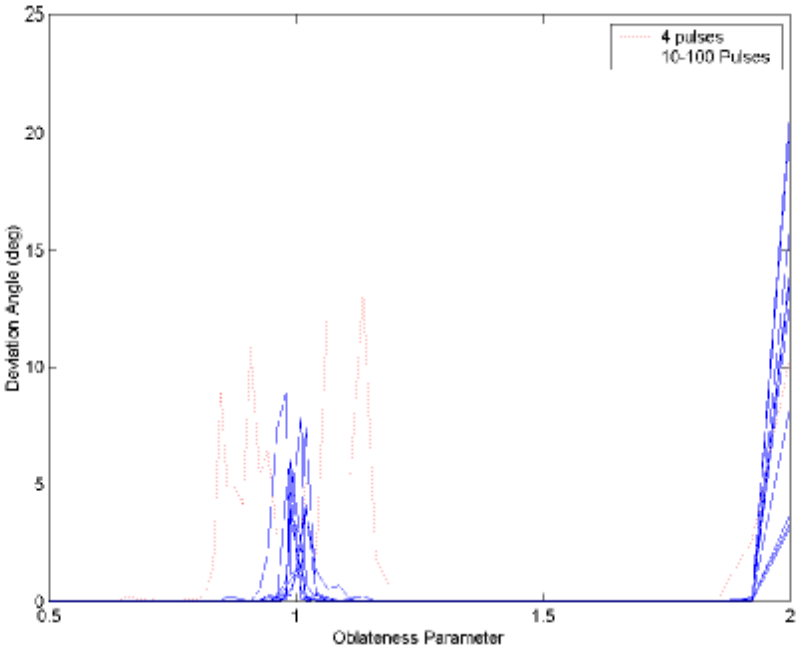

Figure 11 Residual Deviation with Adjusted Pulses, deg

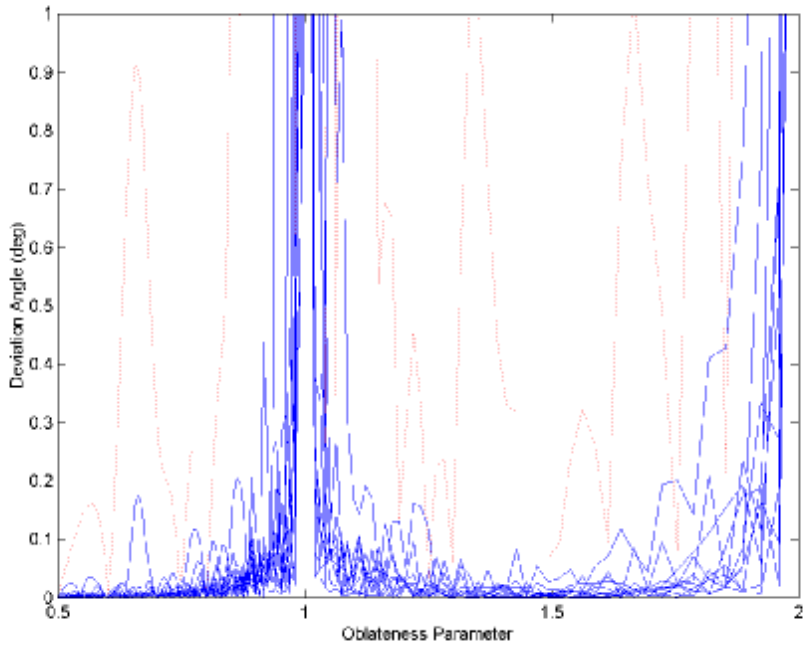

Figure 12 Residual Deviation with Adjusted Pulses (Details), deg

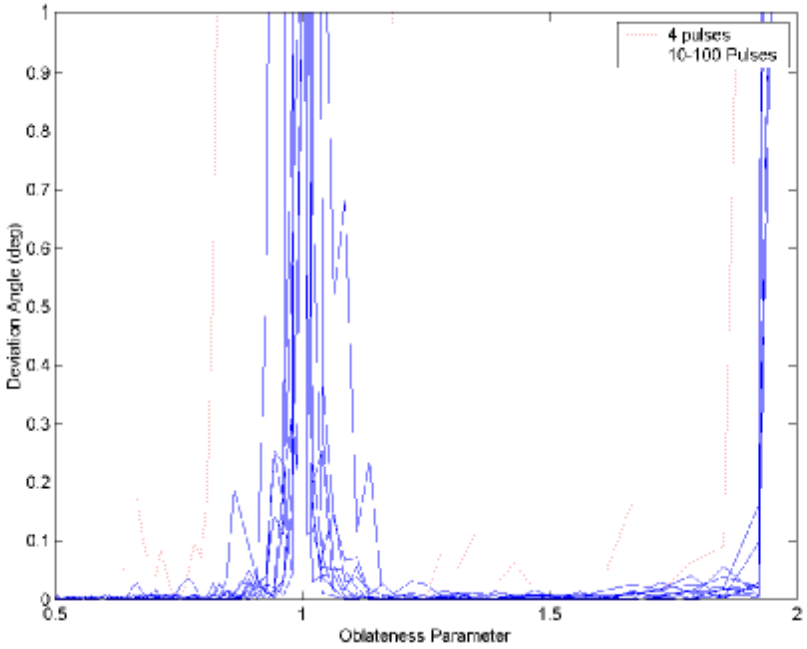

Figure 13 Residual Deviation with Diff. Corrector Adjusted Pulses (Details), deg

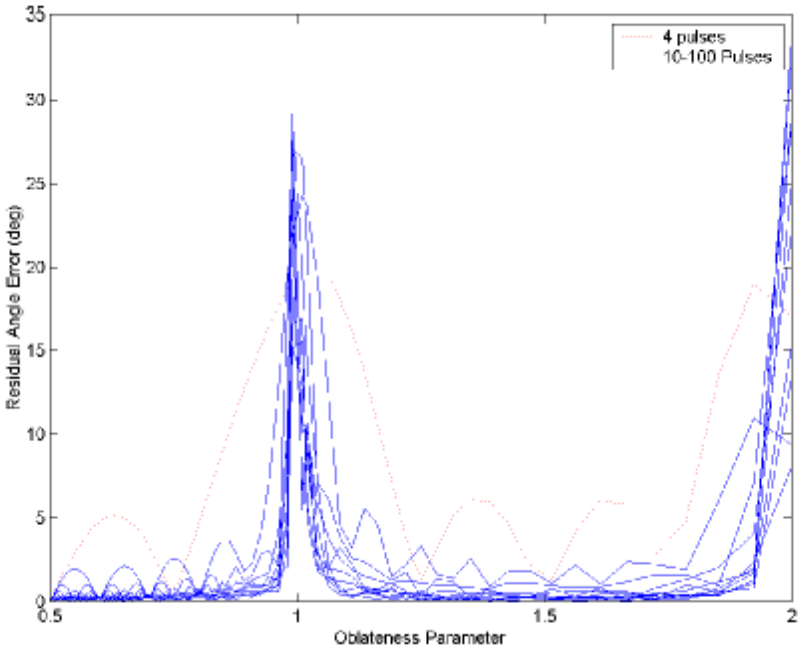

Figure 14 Residual Angle Error with Nominal Pulses, deg

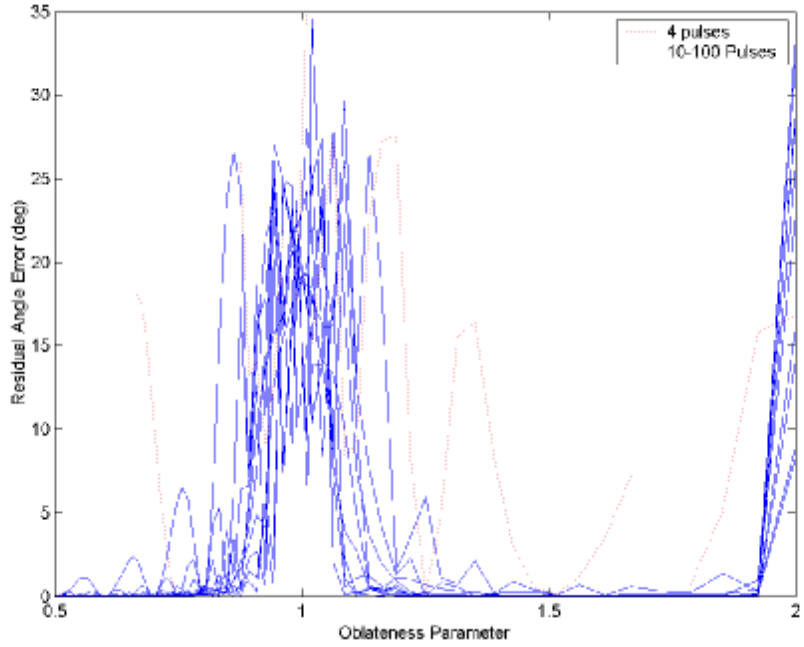

Figure 15 Residual Angle Error with Diff. Corrector Adjusted Pulses, deg

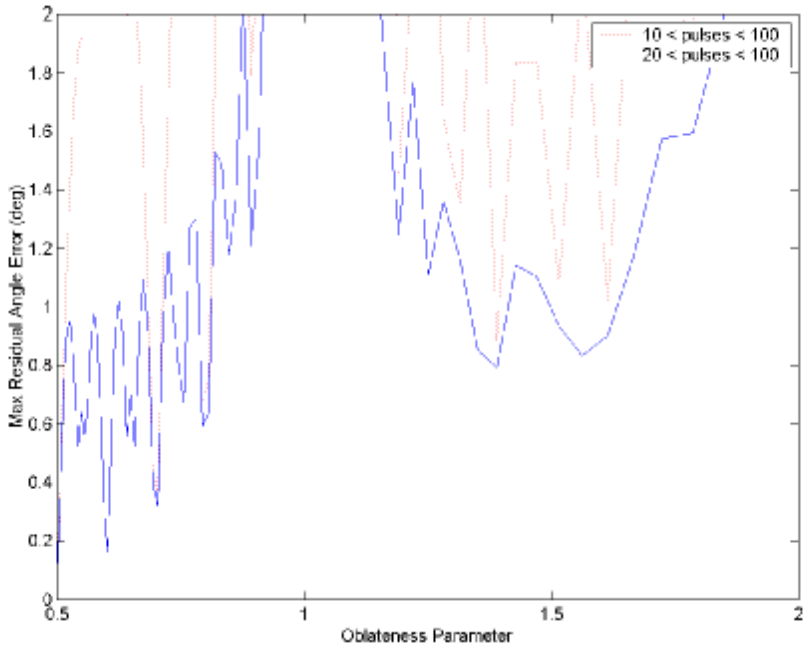

Figure 16 Max Residual Angle Error with Nominal Pulses (Details), deg

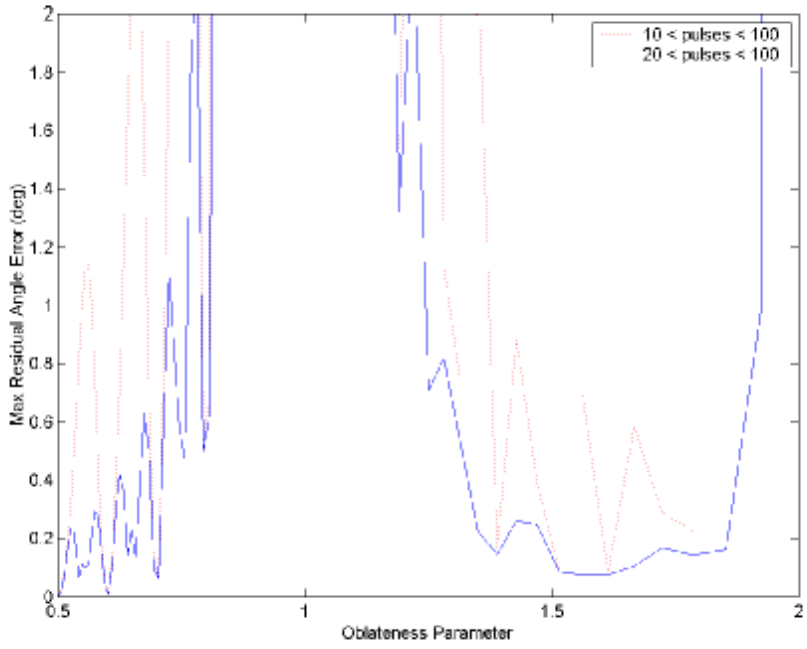

Figure 17 Max Residual Angle Error with Diff. Corrector Adjusted Pulses (Details), deg

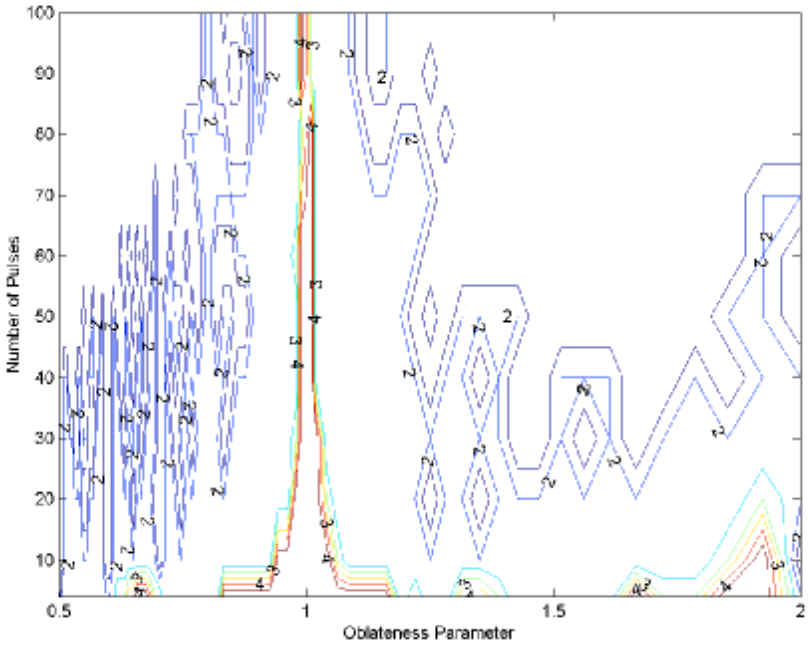

Figure 18 Number of Differential Corrector Iterations, deg

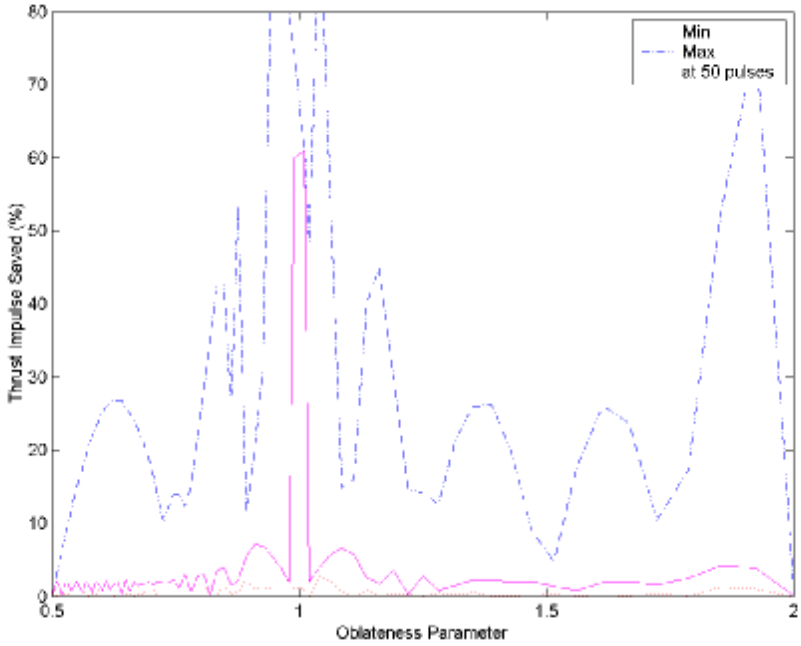

Figure 19 Thrust Impulse Saved, %

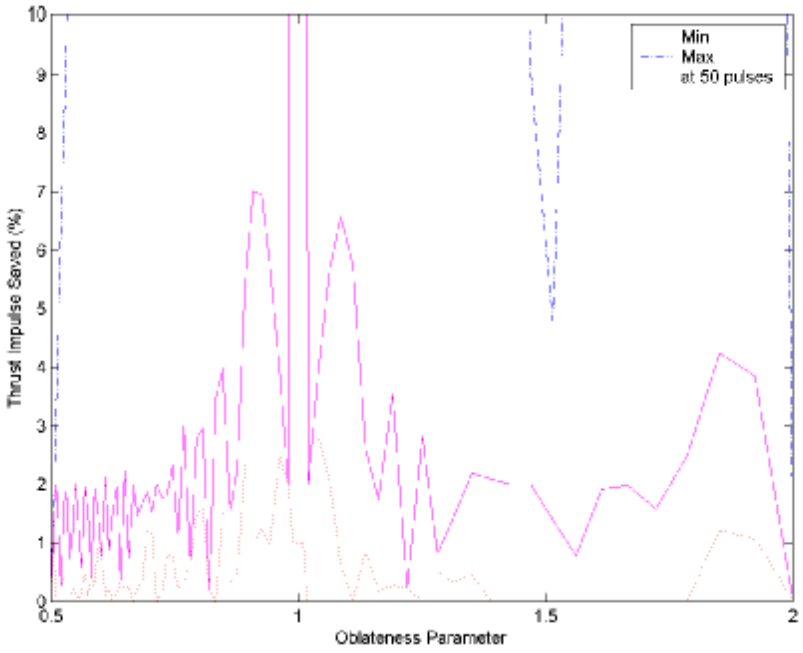

Figure 20 Thrust Impulse Saved (Details), %

TABLE 1. CLOSED-LOOP SOLVER PERFORMANCE IN THE PRESENCE OF MASS PROPERTY IMPERFECTIONS

Oblateness Parameter	Residual Nutation Angle, deg		Residual Deviation Angle, deg	
	Nominal	Adjusted	Nominal	Adjusted
0.8	0.6824	0.3299	0.5013	0.8001
1.2	0.4796	0.1686	0.4790	0.1705
1.7	0.0670	0.0390	0.0978	0.0179

CONCLUSIONS

Examination of several targeting approaches to precession maneuver with simultaneous active nutation control demonstrated their usefulness and efficiency. The approaches generally improve accuracy and have the potential for reducing amount of fuel that would otherwise be needed for post-maneuver active nutation control. In particular, the differential corrector with numerically integrated state and analytic Jacobian exhibits robust behavior at the lowest computational cost. Additional kinematics correction can be applied in some cases in order to further reduce residual deviation from the desired precession plane. Finally, closed-loop solver is proposed, initial study of which indicates its usefulness and robustness with respect to mass property imperfections. However, more investigation is needed to fully evaluate this approach for a wider range of models and initial conditions.

REFERENCES

1. *Spacecraft Attitude Determination and Control*, J.R. Wertz (ed.), Kluver Academic Publishers, 1978.

2. A.E. Bryson, Jr., *Control of Spacecraft and Aircraft,* Princeton University Press, Princeton, NJ, 1994.

3. M.H. Kaplan, *Modern Spacecraft Dynamics and Control*, Wiley, New York, 1976.

4. B. Wie, *Space Vehicle Dynamics and Control,* AIAA Education Series, AIAA, 1998.

5. S. Tanygin and J. Woodburn, "Sensitivity of Spin-Axis Reorientation Maneuvers," AAS Paper 99-321, AAS/AIAA Astrodynamics Specialist Conference, Girdwood, Alaska, Aug. 16-19, 1999.

6. A.C. Or, "Injection Errors of a Rapidly Spinning Spacecraft with Asymmetries and Imbalances," *the Journal of the Astronautical Sciences*, Vol.40, No.3, 1992, pp.419-427.

7. S. Tanygin, "Simultaneous Precession Maneuver and Active Nutation Control," AAS Paper 01-110, AAS/AIAA Space Flight Mechanics Meeting, Santa Barbara, CA, Feb. 11-14, 2001.

8. G.H. Golub and C.F. Van Loan, *Matrix Computations*, 3rd Ed., The John Hopkins University Press, Baltimore, MD, 1996.